NASA TECHNICAL MEMORANDUM

NASA TM X-71466

NASA TM X-71466

EFFECT OF EXHAUST NOZZLE CONFIGURATION ON AERODYNAMIC AND ACOUSTIC PERFORMANCE OF AN EXTERNALLY BLOWN FLAP SYSTEM WITH A QUIET 6:1 BYPASS RATIO ENGINE

by N. E. Samanich, L. J. Heidelberg, and W. L. Jones
Lewis Research Center
Cleveland, Ohio

TECHNICAL PAPER proposed for presentation at
Propulsion Joint Specialist Conference cosponsored by the
American Institute of Aeronautics and Astronautics and
the Society of Automotive Engineers
Las Vegas, Nevada, November 5-7, 1973

EFFECT OF EXHAUST NOZZLE CONFIGURATION ON AERODYNAMIC AND ACOUSTIC PERFORMANCE OF AN EXTERNALLY BLOWN FLAP SYSTEM WITH A QUIET 6:1 BYPASS RATIO ENGINE

by N. E. Samanich*, L. J. Heidelberg*, and W. L. Jones**
V/STOL & Noise Division
Lewis Research Center
National Aeronautics and Space Administration
Cleveland, Ohio

ABSTRACT

A highly suppressed TF-34 engine was used to investigate engine and flap interaction noise associated with an externally blown flap STOL powered lift system. Noise, efficiency, and velocity decay characteristics of mixed and separate flow exhaust systems including convergent, co-annular, and lobed designs were determined with the engine operating alone. Noise data were then obtained for several of the exhaust configurations with the engine blowing a wing-flap segment.

Noise for both the engine alone and the engine with blown flaps showed substantial differences for the various exhaust configurations tested. The differences in observed noise are related primarily to nozzle effective exhaust velocity, flap impingement velocity, and noise spectral shape.

E-7765

INTRODUCTION

The aircraft noise problem is particularly severe for short-haul aircraft operating near heavily populated areas. Because of the relatively small airfields in these areas, aircraft designers are considering some form of supplementary powered lift as a future requirement for these aircraft. Unfortunately, associated with powered lift systems are additional noise sources not present in conventional lifting aircraft. Preliminary investigations

---

*Aerospace Research Engineers, STOL Project Propulsion Office,
**Head, STOL Aircraft Propulsion Section, STOL Project Propulsion Office

indicate that these additional noise sources can be the dominant noise source and may well dictate the choice of the powered lift system.

One method of achieving lift augmentation is the externally blown flap system where the engines are located such that the exhaust gases impinge on (or are directed toward) the wing-flap system and are deflected downward. Lift augmentation comes about by the reaction to the downward jet deflection and also by inducing a favorable pressure distribution on the wing flap system. However, model tests have shown that the interaction of the engine exhaust and the wing-flap system can cause significant noise generation (refs. 1-4). These tests have also shown that the greater the exhaust gas velocity at or near the lifting surface, the greater the noise increase. Engines having low or moderate exhaust velocities are therefore more desirable for this application. However, these engines are, in general, larger and less efficient than higher pressure ratio designs. Consequently, there has been an interest in nozzles that have geometrical characteristics which cause rapid decay of the exhaust velocity so that they could be used with the higher pressure ratio fan engines without generating large increases in flap noise. Nozzles having these characteristics have been designed and tested in small scale as reported in references 5 and 6.

In an attempt to demonstrate the full-scale practicality of a velocity decayer nozzle and also assess the associated acoustic and performance characteristics with a real engine, a 12-lobe nozzle designed for rapid exhaust deceleration (ref. 7) was fabricated and tested with an acoustically suppressed TF-34 turbofan engine (ref. 8). The decayer was tested with and without an acoustically treated shroud and with the core flow discharged internally and in the nozzle exit plane. Other nozzles tested included a co-annular design, and an internally mixed flow convergent nozzle. Only the decayer and co-annular configurations were tested with a wing-flap segment. The results of the tests include nozzle thrust coefficients, exhaust wake surveys, and acoustic characteristics with and without the wing-flap segment.

The tests were conducted at the Edwards Air Force Base with assistance from the NASA Flight Research Center.

APPARATUS AND PROCEDURE

Engine

The TF-34 turbofan engine is a dual-rotor front-fan configuration having a nominal bypass ratio of 6.5. It has a single-stage fan with a pressure ratio of 1.5, and a 14-stage axial-flow compressor with variable stators and nominal pressure ratio of 14.5. The gas generator high pressure turbine has two axial stages, both air-cooled. The fan low pressure turbine has four axial-flow stages and drives the fan through a concentric shaft passing forward inside the gas generator rotor. Air is introduced directly to the fan rotor with no fan inlet guide vanes.

Nacelle

The acoustically treated ground test nacelle used in this test series is schematically shown in fig. 1. The inlet consisted of a bellmouth attached to a cylindrical section housing three splitters. The splitters and walls of the inlet had perforated sheet over honeycomb acoustic treatment.

The main nacelle consisted of the fan exhaust duct and the core engine cowling. The fan duct walls as well as the two fan duct splitters were acoustically treated using perforated face sheet over various thicknesses of a polyurethane open cell foam (Scottfelt 3-900). A main support pylon on top and a narrow pylon on the bottom split the fan duct passage. The core exhaust system consisted of an annular duct lined with two thicknesses of a bulk suppression material (Cerafelt CR-400) held in place by wire screen and a perforated face sheet.

The design of the test nacelle is described in detail in ref. 8, and the noise suppression characteristics of the engine are reported in ref. 9.

Nozzles

The exhaust nozzle systems tested are shown schematically in fig. 2 with dimensional characteristics given in fig. 3. Two basic types were tested, decayer and non-decayer nozzles. A 12-lobe design was selected

for the decayer. The basic decayer is shown in the photograph of fig. 4, and the basis for the design is outlined in ref. 7. Briefly, the number of lobes, their shape and spacing, and the length of the decayer were a compromise between desired velocity decay and minimizing weight and performance loss. The 12-lobed decayer was symmetric except for the "three o'clock" lobe which was trimmed to a smaller radius to enable closer placement to a wing surface. Aerodynamically shaped inserts were used for modifying the exit area of the decayer from 1050 in.^{2} to 927 in.^{2}. An 8.0 in. radius centerbody extended aft from the turbine and closed with a low angle plug downstream of the decayer exit. The decayer was tested with the core flow discharged internally with a conic nozzle (fig. 2(d); conic-decayer) and with a daisy-type mixer (fig. 2(a); mixer-decayer). The mixer forms a smooth transition from a 280 in.^{2} annular passage to 12 symmetric lobes around the centerbody having an exit area of 250 in.^{2}. The mixer lobes were oriented in-line with the decayer lobes.

A modification of the basic decayer to a separate flow system was made by extending the annular core passage and separating it from the fan flow by sheet metal inserts in the decayer lobes. Flow straightening visors were also added in the exit plane of this configuration (fig. 2(e); co-planar decayer). This decayer configuration was also tested with a 6-foot long shroud (fig. 2(f)) with the leading edge located 18 in. ahead of the fan visor-trailing edge. The shroud had a 3 in. thick layer of a bulk suppression material (Cerafelt CR-400) covered by a perforated skin 22 percent open with .03 in. diameter holes. Other configurations tested include a convergent nozzle with the core flow discharged internally using both the 12 lobe core mixer (fig. 2(b); mixer-conic) and the annular core nozzle (fig. 2(c); conic-conic). A separate flow co-annular nozzle (fig. 2(g)) was used as a reference in the suppressed TF-34 tests. Performance data with the unsuppressed TF-34 and typical flight type cowling (fig. 2(h)) was also obtained.

The wing segment used in the test was based on the full wing design given in fig. 5(a). The nominal airfoil at the root is a NACA 63_2A214 section, and at the tip it is a NACA 63_2A211 section. The ordinates at and

forward of the trailing edge were modified to provide a finite trailing edge thickness and to fair in the flap system.

Wing flaps are triple-slotted full span flaps with a .15, .20, and .225 percent local wing chord for the first, second, and third elements respectively (fig. 5(b)). The first flap element is a 15 percent wing local chord St Cyr 178 modified to .0065 t/c at the trailing edge. The second flap element is a St Cyr 178 airfoil modified slightly to facilitate flap nesting in the undeployed configuration and to provide a finite trailing edge thickness. The third flap element is a NACA 4412 section modified to .0045 t/c at the trailing edge. All flap slot heights are .015 wing local chord.

Test Facility

The test facility is located on the edge of Rogers Dry Lake at Edwards Air Force Base. A photograph of the test installation with engine and wing assembly is shown in fig. 6. A gallows structure supports the engine above a steel base plate which is suspended by four flexure plates below ground level. Thrust is measured at the forward end of the base plate by a load cell. The engine was mounted with its horizontal centerline nine feet above a flat concrete and steel surface. The position of the engine with respect to the wing could be varied. This test facility is at an altitude 2300 ft. above sea level.

Instrumentation

Far-field acoustic data were recorded by 17 microphones spaced every 10 degrees from 0 to 160° on the arc of a 100-ft. radius (simulated flyover measurements). The center of the arc lies in the center of the exhaust nozzle exit plane. Zero degrees is taken from the engine centerline in front of the engine, counterclockwise looking down from above. The microphones were in the same horizontal plane as the engine centerline. No corrections were made for ground cancellations or re-enforcements. In addition, a portable tower was used to mount a microphone 50 ft. above the nozzle exit plane (fig. 6) for simulated sideline noise measurement.

The locations of the various engine instrumentation stations are shown in fig. 1. Total airflow was calculated from pressure and temperature measurements along with the known flow area at the bellmouth throat (station 1). Similar measurements at the core inlet (station 2c) were used to calculate core flow. Four 5-element rakes at station 2 and eight 5-element total pressure rakes behind the fan (station 24) were used to determine fan pressure ratio. Speed sensors were used to measure fan and core speeds. Engine instrumentation was also located at the core compressor outlet (station 3) and at the entrance (station 5.4) and outlet of the low pressure turbine (station 6). Pressure surveys were made behind the fan duct splitters (station 25) and in the core duct passage aft of the treatment (station 7). All survey rakes in the inlet and fan and core exit passages were removed when far-field acoustic measurements were made. More details of the instrumentation are presented in ref. 8.

Exhaust wake surveys were made with a portable 48-in. long rake. Twenty-four combination total pressure and temperature probes were located every two inches. Between the combination probes were 24 static pressure elements.

Test Procedure

Tests were conducted only if the wind speed was under 5 mph and were stopped if the wind speed exceeded 7 mph. The engine was allowed to stabilize for two minutes at each power setting before data were taken. For far-field acoustic runs, the engine was run at five different power settings covering the range from maximum power to approximately half power. The rated power setting corresponds to a low-pressure turbine inlet temperature, ($T_{5.4}$) of 1955° R, and the corresponding maximum fan speed was determined by ambient temperature. The other four power settings correspond to mechanical fan speeds of 6500, 6200, 5800, and 5100 rpm. Ambient conditions of wind velocity, temperature, pressure and relative humidity were measured for all runs.

AERODYNAMIC PERFORMANCE

Exhaust Surveys

Exhaust velocities were calculated from total pressure, static pressure, and total temperature measurements made with the survey rake and from isentropic gas dynamic relationships. The rake was located in three positions with respect to the engine centerline for the decayer nozzles as well as several distances downstream of the exit plane. Visual as well as rake survey data of the mixer-decayer and conic-decayer nozzles indicated the core flow to have a significantly large, radial velocity component at the decayer exit. A region of local flow separation appeared to exist at the inner portion of the lobes and the engine centerbody. A schematic representation of the flow field at the exit of a lobe of the mixer-decayer nozzle is shown in fig. 7.

A summary of the velocity decay results obtained with the various nozzles tested is given in fig. 8, where the peak measured velocity is shown at various distances behind the nozzles. As would be expected, the non-decayer nozzles had very little decay compared to the others. The mixer-conic did, however, have a fairly rapid rate for the first 40 in. with little decay after that. The mixer-decayer and the conic decayer (both large and small area) nozzles had peak velocities at the nozzle exit that were substantially greater than the peak velocity from the co-annular or conic-conic nozzles

Although exit plane date indicated somewhat better hot gas mixing internally with the mixer, none of the decayer configurations had any significant degree of internal mixing. However, rapid external mixing occurred with both configurations and very flat velocity profiles were measured 100 in. from the exit. The decayer was designed to reduce the exhaust velocity 38 percent in 115 in. (3 equivalent nozzle diameters). Measurements showed considerably greater velocity reductions were attained (around 50% for average velocity, and around 65% for peak velocity).

The co-planar decayer had relatively flat profiles in the exit plane, with the core flow velocity about 150 ft/sec greater than the fan flow velocity

at rated power. The core velocity diminished to about the same value as the fan flow velocity at low power settings. The velocity decay rate with or without the shroud was similar.

Peak exhaust gas temperature decay is presented in fig. 9. All decayer and mixer configurations had rapid temperature decay (only the decayers had rapid velocity decay). The conic-conic showed very little gas mixing, while the co-annular nozzle maintained a hot core for 115 in. and mixed rapidly beyond that. The most significant difference in velocity and temperature decay rates occurred with the mixer-conic nozzle. Although the velocity decayed only modestly (fig. 8), the mixer did cause a very rapid core gas mixing as can be seen in fig. 9 as compared to very little temperature mixing without the internal mixer (conic-conic).

Exhaust Nozzle Efficiency

An attempt was made to arrive at the thrust loss associated with the nozzle configurations tested. The measured thrust of the engine-nozzle assembly was ratioed to the sum of the ideal momentum of the fan and core streams calculated from gas properties and weight flows at stations 25 and 7, respectively (fig. 1). The thrust coefficient obtained in this manner is shown in fig. 10 as a function of fan pressure ratio. Also shown for comparison are the values obtained with the flight-type cowling. All of the systems appeared to have efficiencies that were insensitive to fan pressure ratio over the range tested. The greatest efficiency was measured with the unsuppressed flight-type exhaust system having a value of about 0.99 (top line). The co-annular exhaust was about 3 counts lower (middle line). It is speculated that this lower efficiency is a result of attempting to minimize the exhaust nozzle length with a short fan cowl and steep (25^{o}) fan discharge angle. In addition, wake survey data did indicate a sizeable flow separation existing immediately downstream of the large external bullet.

All of the decayer configurations had thrust losses 3-5 percent greater than the co-annular nozzle. This additional thrust loss was due to additional wall friction (estimated to be ~1 percent), base pressure forces on the

bullet and outer surfaces of the decayer, and mixing and flow angularity losses with the mixed flow decayer nozzles. The placement of the shroud over the co-planar decayer resulted in an additional 1-2 percent thrust loss (bottom line). The position of the shroud was dictated to a great degree by the on-site mounting structure. It is speculated that if the shroud leading edge were located slightly aft of the nozzle exit, a sizeable static thrust augmentation would be realized. In the position tested with the shroud leading edge 18 in. ahead of the fan visor exit, the thrust loss was 1% less when the acoustic treatment was taped (simulation of hard-walled shroud). The conic-conic and mixer-conic nozzles had the highest measured efficiencies (~.985) with the suppressed nacelle. There was no apparent thrust advantage with the use of the internal mixer compared to an internal annular core nozzle as measured with both the convergent and decayer nozzles.

ACOUSTIC RESULTS

Engine Alone

The maximum perceived noise level (PNL) at 500-foot (sideline or flyover) for the engine alone with the various exhaust systems are compared in fig. 11. The PNL is presented as a function of the measured engine thrust for each exhaust system. The rated thrust which is the thrust obtained at a comparable power setting (low-pressure turbine inlet temperature of 1955^{o}R) is also shown for each configuration.

The top curve is the unsuppressed flight-type configuration of the TF-34. The suppressed TF-34 configuration with the co-annular nozzle was used in evaluating the effect of the acoustic treatment (ref. 9). A 15-17 PNdB noise reduction from the unsuppressed engine noise level was measured at comparable thrust levels, but the rated thrust was about 14 percent lower with the suppressed nacelle.

The mixed-flow decayer configurations were 8-11 PNdB louder than the co-annular nozzle. The co-planar decayer was from 1 to 5 PNdB louder than the co-annular at low and high power settings, respectively. However,

the addition of the acoustic shroud reduced the PNL by 3-4 PNdB for this nozzle. The mixer-conic was the quietest configuration, being about 1 PNdB lower than the co-annular nozzle configuration.

The acoustic comparisons of fig. 11 were made on an engine thrust basis. Unfortunately, some of the nozzles had sizeable effects on the engine cycle and operating line which made it difficult to assess whether the noise characteristics measured were truly representative of the basic exhaust nozzle concept. The observed trends of maximum PNL as obtained in fig. 11 must therefore be examined with respect to differences in exhaust velocity, spectral shape and directivity pattern for each configuration.

Sound Level Correlations

An attempt was made to correlate the noise levels with an area weighted effective exhaust velocity, based on a power velocity dependence, such that

$$\bar{V}_n = \sqrt[n]{\frac{V_F^n A_F + V_C^n A_C}{A_F + A_C}} \qquad (1)$$

where A_F and A_C = fan and core exit areas, and V_F and V_C = fan and core ideal isentropic exhaust velocities.

Since the aft quadrant noise was believed to be predominantly jet noise (ref. 9), n was taken as 8. Because all of the nozzles had little or no internal mixing of the fan and core streams, except the mixer-conic, it was felt that this velocity might be a reasonable correlating parameter for the nozzle alone noise. The mixer-conic had approximately 50-60 percent internal mixing based on a thrust potential basis and the effective velocity for jet noise correlation is probably somewhere between the eight power (eq. (1)) and completely mixed or mass-weighted-velocity, which was also calculated.

The overall sound pressure level (OASPL) normalized with respect to nozzle exit area is presented as a function of the acoustic effective exhaust

velocity, $\overline{V}_8$, in fig. 12 at about the peak noise location (130° from the inlet). The mixer-conic noise levels correlate better assuming a mass average exhaust velocity, indicating significant internal mixing, rather than assuming the no-mixing eighth power velocity, $\overline{V}_8$ (eq. (1)). All further discussions in this paper pertaining to the mixer-conic nozzle will use the mass average exhaust velocity as the acoustic effective velocity.

The co-planar decayer with shroud configuration has somewhat lower noise levels than the other nozzles, as might be expected due to acoustic energy absorption from the jet exhaust by the shroud treatment. Excluding this configuration, the noise levels correlate quite closely for all the nozzle types with a maximum spread of 2 dB. The data shows an approximate 7th power velocity dependence, indicating a slight influence of noise sources other than that from the jet exhaust at this angular position.

The overall normalized sound power level (PWL) correlation is presented for the various exhaust systems in fig. 13 as a function of acoustic effective velocity. The co-annular exhaust configuration (solid line) has a power level somewhat higher than the other configurations. However, all appeared to merge at lower effective velocities. The power level of the acoustically-treated shroud configuration at the higher effective exhaust velocities was about 2 dB lower than the decayer alone, suggesting that a significant amount of the noise benefit obtained with the shroud was due to energy absorption. Tests with the shroud treatment taped indicated that about 2/3 of the noise reduction with the shroud was due to acoustic treatment. The data showed an approximate 6th power velocity dependence for velocities greater than 600 ft/sec. This indicates an influence from noise sources such as the inlet which have a lower power velocity dependence than the jet exhaust.

Effective exhaust velocity. - Since the OASPL and PWL correlated well with the eighth-power effective exhaust velocity, but large differences in noise were observed at comparable thrust levels, it was not surprising to see large variations in exhaust velocity for the various nozzle types. Fig. 14 shows the variation in effective exhaust velocity with thrust for the test nozzles. Very substantial differences were obtained for the different nozzles,

which relate approximately to the corresponding differences in noise level (fig. 11).

The mixed-flow decayer nozzles having the loudest PNL's (fig. 11), are seen to have the highest effective exhaust velocities. The quietest configurations likewise, had the lowest exhaust velocities. About 75 percent of the observed differences in perceived noise levels between the co-annular configuration and the decayer nozzles in fig. 11 can be accounted for by differences in effective exhaust velocity. (The exhaust velocity of the unsuppressed engine with flight cowling is also presented for comparison in fig. 14, but should not be used to correlate with its noise levels because fan, not jet noise, was the dominant noise source for that configuration.)

The results of fig. 14 indicate that a significant consideration in the design of a particular exhaust nozzle configuration should be the potential effect of the nozzle on the effective exhaust velocity.

Spectral variations. - The remainder of the difference in PNL among the nozzles tested appears to be the result of spectral variations and not directivity characteristics, since the peak noise occurred at comparable azimuthal angles ($\theta = 110^{\circ} - 120^{\circ}$) in all cases. The case for spectral variations can be deduced from the data presented in the next two figures. The normalized maximum PNL along a 500-foot sideline is shown for the various configurations in fig. 15. The correlation is different that the OASPL data at a constant radius presented in fig. 12. The co-annular nozzle (solid line) is now the quietest on a perceived noise basis, as compared to being the loudest on an overall sound power level basis (fig. 13).

The mixer-decayer was the quietest of the decayer configurations, but was 1 to 2 dB louder than the co-annular nozzle. The co-planar decayer was about 3 dB louder than the co-annular but became the same as the co-annular when the acoustic shroud was added. The shrouded decayer was about 2 and 4 PNdB quieter than the unshrouded decayer at low and high effective exhaust velocities, respectively.

Sound pressure level (SPL) spectrum are presented for most of the nozzles in fig. 16. The data were selected from power settings where the effective exhaust velocities were similar. Two of the loudest nozzles, the

co-planar decayer and mixer-decayer had similar spectra. Although these two nozzles had the lowest SPL's up to 630 Hz, they were significantly higher than the co-annular above that frequency where the annoyance factor is greater. Of the two, the slightly quieter mixer-decayer nozzle has lower SPL's below 200 and above 4000 Hz. The shift in the frequency at which the peak SPL occurs between the co-annular and the decayer nozzles is about a factor of 10 and is proportional to the ratio of the characteristic dimensions of the two nozzle geometries (37.0 in. effective diameter and 3.7 in. lobe slot height, respectively).

Spectra comparisons with and without the acoustic shroud indicate that the shroud absorbed energy primarily in the 630 to 10,000 Hz region. At the lower exhaust velocities, the shroud removed a comparable amount of energy in the same frequency band. However, an increase of about 5 dB's in SPL was observed at low frequencies (to 315 Hz). This low frequency increase offset some of the acoustic benefits of the shroud and resulted in a smaller perceived noise reduction (2 PNdB at low compared to 4 PNdB at high effective exhaust velocities). The mixer-conic, the quietest nozzle, had about 4 dB lower SPL's in the low frequency range (to 400 Hz) compared to the co-annular nozzle and only sightly lower values (~ 1dB) at the higher frequencies.

Engine with Blown Flap

Four nozzle configurations were tested with the engine exhaust blowing against the wing-flap segment. They were: the mixer-decayer; the co-planar decayer; the co-planar decayer with shroud; and the co-annular. The orientation of the engine exhaust with respect to the wing system is shown in fig. 17. This arrangement was established from NASA Langley wind tunnel tests of a high-lift four engine STOL transport configuration. Somewhat lower engine locations were tested with the decayer nozzles because of interference between the nozzles and wing structure. The orientations tested are tabulated on the figure.

Perceived noise levels. - A comparison of the maximum perceived noise levels for the various exhaust nozzles for the different flap configurations

tested is made in fig. 18. The mixer-decayer was tested with only the 40^{o} flap position. The loudest flyover noise was measured with the co-annular nozzle for the 55^{o} flap position with a peak PNL of 105 PNdB at 7200 lbs. thrust. For the 40^{o} flap position and 7200 lbs thrust, the measured PNL's were 104, 101 and 97 respectively, for the co-annular, co-planar decayer and co-planar decayer with shroud. The mixer-decayer was about as noisy as the co-annular nozzle for the 40^{o} flap, and for the retracted flap configuration the co-planar decayer nozzle was about as noisy as the co-annular nozzle. The addition of the shroud to the co-planar decayer nozzle decreased the PNL by around 3 PNdB for all flap angles.

The maximum perceived noise level in a 500-foot flyover is presented individually for each of the four configurations in fig. 19. For each nozzle configuration, the PNL is presented against thrust for the retracted, 0-20-40^{o}, and 15-35-55^{o} flap settings along with the engine alone data. As would be expected, the co-annular nozzle produced the largest increase in flyover perceived noise, with increases of about 4, 12 and 13 PNdB for the 0, 40 and 55^{o} flaps, respectively. All of the decayer configurations had an increase of about 4-5 PNdB for both the 40 and 55^{o} flaps. The incremental noise increases were almost constant over the range of thrust values for all of the configurations.

The increase in noise compared to the engine alone case for the retracted flap configuration is due to scrubbing noise and trailing edge noise resulting from the exhaust flow over the lower surface of the wing and from downward reflection of engine exhaust noise. With the flaps deflected, the further increase in noise results from the flow over the flap surfaces and trailing edges, plus some reflection of the engine exhaust noise by the flaps. For the decayer nozzles, both wing and flap noise increments are less than those for the co-annular nozzle because of the lower levels of velocity at the wing and flaps with the velocity decayer nozzles (e.g., fig. 8). The absolute level of the noise for a given flap position then depends on the noise level of the engine-alone for these decayer nozzle configurations. As indicated earlier, the noise levels for the engine-alone depended primarily on the effective exhaust velocity of the particular nozzle configuration.

Correlations. - Analyses of cold-flow and engine externally blown flap data have indicated that flap noise is proportional to the 6th power of the nozzle exhaust velocity for configurations have a negligible velocity decay. In the current tests, the co-annular nozzle had essentially the same velocity at the flaps as in the exit plane. However, the velocity at the flaps for the decayer nozzles was substantially less than the calculated effective exhaust velocity in the exit plane.

Nozzle-area normalized OASPL is presented in fig. 20 in terms of 6th power effective exhaust velocity (eq. (1) with n = 6) with the engine blowing the 40° flaps. The noise levels are shown 80° from the inlet, the angle at which the maximum PNL occurred along a 500-foot flyover for the co-annular nozzle. The decayer nozzles had significantly lower OASPL's than the co-annular nozzles because of the low impingement velocities involved. The decayer nozzles without the shroud, collapsed on one curve, while the decayer with shroud was only 1 dB lower. Also shown on the figure is the good agreement between measured OASPL and the estimated value for the co-annular nozzle based on ref. 10.

Probably of more direct interest is the maximum perceived noise level in a 500-foot flyover which is presented in fig. 21. The data again show a good correlation of the non-shrouded decayer nozzles, suggesting similar noise spectra. However, the incremental PNL variations between the nozzle types is significantly different from those observed in the OASPL's in the previous figure indicating different spectra shapes or directivity characteristics.

Directivity. - The acoustic directivity characteristics for the engine alone are compared to results with the 40° flap in a 500-foot flyover in fig. 22 at comparable $\overline{V}_6$ effective exhaust velocities. The trends are similar for all the nozzles, with the peak noise occuring at an azimuthal angle of $110\text{-}120^{\circ}$ for the engine alone and moving forward to $100\text{-}110^{\circ}$ for the decayer configurations and to 80° for the co-annular when blowing against the flap. Similar directivity characteristics were measured at other exhaust velocities.

Spectra. - The sound spectra at the locations where the maximum PNL occurred for engine alone and when blowing against the 40° flaps are presented in fig. 23. All the decayer configurations show the increase in SPL when

blowing the flaps to be predominant at frequencies below 400 Hz and considerably less above that. However, in addition to a similar low frequency SPL increase, the co-annular nozzle (fig. 23 (d)) had significant increases over the entire frequency range.

The estimated flap noise spectrum from ref. 10 is compared for the co-annular nozzle (fig. 23 (d)) and the co-planar decayer nozzle (fig. 23 (b)). The predicted SPL agrees well with the co-annular nozzle data and is significantly higher than that obtained with the engine alone, indicating further that the entire spectrum level is predominantly flap generated noise. The dashed line in fig. 23(b) indicates that the decayer configuration with the low impingement velocities (~300 ft/sec) appear to have only a small flap noise contribution to the spectrum at frequencies less than 250 Hz (fig. 23(b)). At higher frequencies, the SPL level appears to be controlled by a re-direction and/or reflection of the engine exhaust noise.

The one-third octave band spectra for the four nozzle configurations are compared at similar effective velocity levels for the 40^{o} flap case in fig. 24. The co-annular nozzle has a considerably higher SPL content over the lower frequency range due to its higher flap impingement velocity. The decayer configurations (low impingement velocities) have quite similar spectra, except for the noticeably lower SPL's above 630 Hz with the shrouded decayer.

As seen earlier in the engine alone data, the reduction in SPL in the 500 to 10 000 Hz frequency range caused by the addition of the shroud (fig. 16) resulted in a reduction of 4 PNdB at high effective exhaust velocities (fig. 15). A similar reduction in SPL in the same frequency range is observed when blowing the 40^{o} flap with the shrouded compared to the unshrouded decayer in figure 24 which resulted in a comparable reduction in PNL (fig. 21). A similar situation was observed at a low power setting. This suggests again that the overall PNL with the decayer configurations at the high exit velocities is dominated by engine exhaust noise rather than flap noise.

Sideline relief. - The most extensive acoustic measurements were made in the flyover plane. However, limited data were obtained directly off the wing tip by boom microphones (fig. 6). The data are summarized in fig. 25 in terms of perceived noise level. The sideline relief values are the difference between the maximum PNL measured in the 500-foot flyover plane and the value obtained by the wing tip microphone, extrapolated to a distance of 500 feet. The sideline relief values were essentially independent of exhaust velocity level over the range tested. The data indicate similar slopes as flap angle is varied for all the nozzles. However, the relief for the noisiest configuration, the co-annular nozzle, was 2 to 3 PNdB more than the decayer configurations.

The sound spectra off the wing tip is compared to the flyover plane values for the co-annular nozzle blowing the 40° flaps is shown in fig. 26. The engine alone data are also presented as measured with the boom microphone. The data indicate the sideline relief to result predominantly from lower values of SPL at frequencies up to 3150 Hz.

Concluding Remarks

A cursory test program was conducted using a highly noise suppressed TF-34 engine with various exhaust nozzle configurations blowing against a wing and triple flap segment to establish full scale flap noise magnitudes. Co-annular as well as velocity decayer nozzle designs were tested. Thrust and noise characteristics of mixed exhaust flow systems were compared to separate flow systems.

When blowing the wing with 40° flaps at near rated power setting (7200 lb static thrust), the maximum PNL in a 500-foot flyover was 104, 101, and 97 PNdB with the co-annular, decayer, and decayer with shroud configurations, respectively. In general, it was found that overall system noise was determined by nozzle exhaust velocity, flap impingement velocity, and noise spectral shape. A 12 PNdB increase measured when blowing the flaps with the co-annular nozzle was predominantly flap generated noise.

The decayer tested was designed to reduce the exhaust velocity 38 per-

cent in 3 equivalent nozzle diameters, but measurements showed that considerably greater velocity reductions were attained (around 50 percent in average and 65 percent in peak). In addition, a significant increase in nozzle exhaust velocity and a thrust loss of about 4 percent was measured for the decayer nozzles. As a consequence, the perceived noise level of the engine was significantly louder with the decayer nozzles than with the co-annular nozzle at comparable thrust levels. Even though the flap impingement velocities were less than 400 ft/sec with the decayer nozzles, some low frequency noise was generated when blowing the flap system. However, the 4 to 5 PNdB increase with flap blowing obtained with all of the decayer configurations was due predominantly to a redirection and reflection of the exhaust system noise by the wing-flap system.

The test results also indicated that for the configurations tested, no apparent thrust advantage appeared to exist with the use of an internal mixer. However, the jet noise level appeared to be about the quietest with the internal mixer and convergent circular nozzle.

It is believed that a revised decayer nozzle could be designed for a more moderate decay rate with considerably less thrust loss and jet noise. A design having better internal mixing with a decayer having fewer lobes of lower aspect ratio and better aerodynamic contours would contribute much to reduce internal losses. A revised lobe design might also reduce peak-frequency shift to minimize the effect on perceived noise. When considering that the decayer nozzles tested actually showed a small decrease in sound power level compared to the co-annular nozzle (based on calculated effective exhaust velocity), it is conceivable that a modified decayer design might have a significantly improved noise characteristic. It should therefore, be possible to obtain an optimum decayer design for reducing flap noise with small thrust loss and very little, if any, jet noise penalty.

References

1. Dorsch, R. G., Krejsa, E. A., and Olsen, W. A., "Blown Flap Noise Research," Paper 71-745, June 1971, AIAA, New York, N. Y.

2. Dorsch, R. G., Kreim, W. J., and Olsen, W. A., "Externally Blown Flap Noise," Paper 72-129, Jan. 1972, AIAA, New York, N. Y.

3. Olsen, W. A., Dorsch, R. G., and Miles, J. H., "Noise Produced by a Small-Scale Externally Blown Flap," TN D-6636, 1972, NASA, Cleveland, Ohio.

4. Dorsch, R. G., Lasagna, P. L., Maglieri, D. J., and Olsen, W. A., "Flap Noise," Aircraft Engine Noise Reduction, SP-311, 1972. NASA, Washington, D. C., pp. 259-290.

5. von Glahn, U. H., Groesbeck, D. E., and Huff, R. G., "Peak Axial-Velocity Decay with Single- and Multi-Element Nozzles," Paper 72-48, Jan. 1972, AIAA, New York, N. Y.

6. Goodykoontz, J. H., Olsen, W. A., and Dorsch, R. G., "Small-Scale Tests of the Mixer Nozzle Concept for Reducing Blown Flap Noise," TM X-2638, 1972, NASA, Cleveland, Ohio.

7. Chamay, A., Edkins, D. P., Mishler, R. B., and Clapper, W. S., "Design of a TF-34 Turbofan Mixer for Reduction of Flap Impingement Noise," NASA CR-120916, Feb. 1972, General Electric Co., Lynn, Mass.

8. Edkins, D. P., "Acoustically Treated Ground Test Nacelle for the General Electric TF-34 Turbofan," NASA CR-120915, Jan. 1972, General Electric Co., Lynn, Mass.

9. Jones, W. L., Heidelberg, L. J., and Goldman, R. G., "Highly Noise Suppressed Bypass 6 Engine for STOL Applications," Paper 73-1031, Oct. 1973, AIAA, New York, N. Y.

10. Clark, B. L., Dorsch, R. G., and Reshotko, M., "Flap Noise Prediction Method for an Externally Blown Flap System," Paper 73-1028, Oct. 1973, AIAA, New York, N. Y.

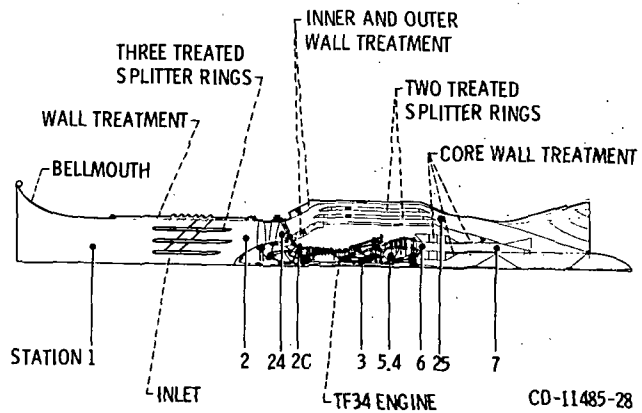

Figure 1. - Schematic of acoustically treated nacelle with engine station designation.

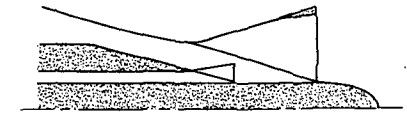

(a) MIXER-DECAYER

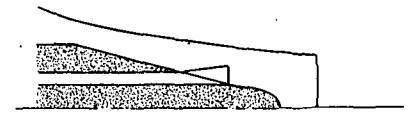

(b) MIXER-CONIC

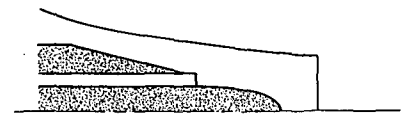

(c) CONIC-CONIC

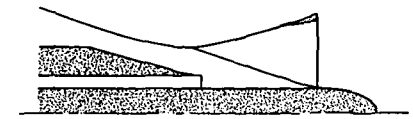

(d) CONIC-DECAYER

MIXED FLOW CONFIGURATIONS

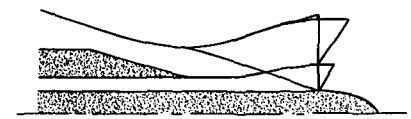

(e) CO-PLANAR DECAYER

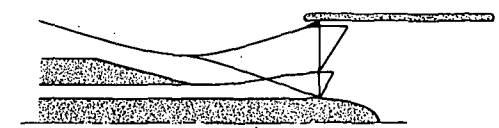

(f) CO-PLANAR DECAYER WITH SHROUD

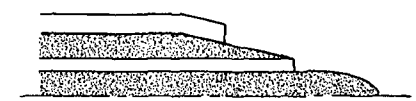

(g) CO-ANNULAR

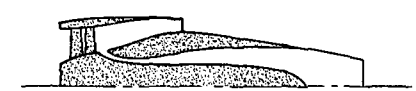

(h) FLIGHT COWLING

SEPARATE FLOW CONFIGURATIONS

Figure 2. - TF-34 exhaust nozzle configurations.

CONFIGURATION	DIMENSION						EXIT AREA, IN.^{2}	
SEPARATE FLOW EXHAUST	α	L_1	L_2	R_1	R_2	R_4	A_8	A_{28}
CO-PLANAR-DECAYER	---	----	20.3	33.1	17.9	8.0	295	815
CO-PLANAR-DECAYER W/SHROUD	---	----	20.3	33.1	17.9	8.0	295	815
CO-ANNULAR	25^0	27.0	29.0	24.9	12.4	8.0	280	790
FLIGHT COWLING	4^0	80.0	----	24.0	8.2	---	209	657

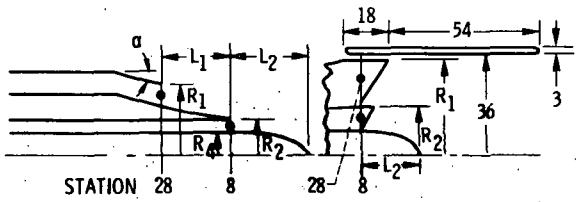

(a) SEPARATE FLOW NOZZLES.

CONFIGURATION	DIMENSION						EXIT AREA, IN.^{2}	
MIXED FLOW EXHAUST	L_2	L_3	R_3	R_4	R_5	R_6	$A_{7.7}$	A_8
MIXER-DECAYER	20.3	28.0	15.4	8.0	32.0	35.0	250	1049
MIXER-CONIC	----	28.0	15.4	8.0	18.8	----	250	1104
CONIC-CONIC	----	40.0	12.0	8.0	18.8	----	250	1104
CONIC-DECAYER	20.3	37.7	12.4	8.0	32.0	35.0	280	1049
CONIC-DECAYER (SMALL)	20.3	37.7	12.4	8.0	29.8	35.0	280	927

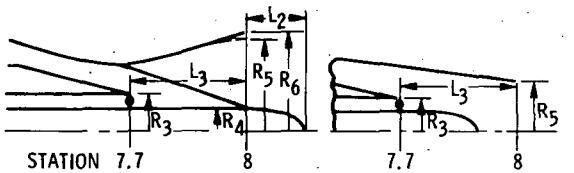

(b) MIXED FLOW NOZZLES.

Figure 3. - Exhaust nozzle dimensions (in.).

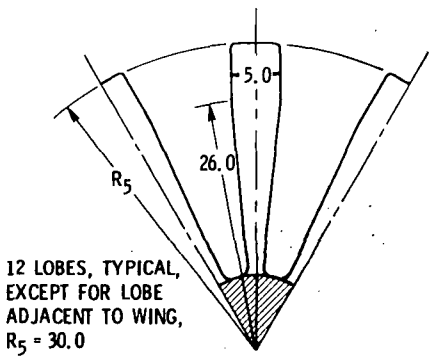

DECAYER EXIT PLANE

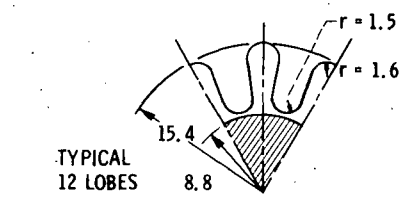

MIXER EXIT PLANE

(c) DECAYER AND INTERNAL MIXER LOBE.

Figure 3. - Concluded.

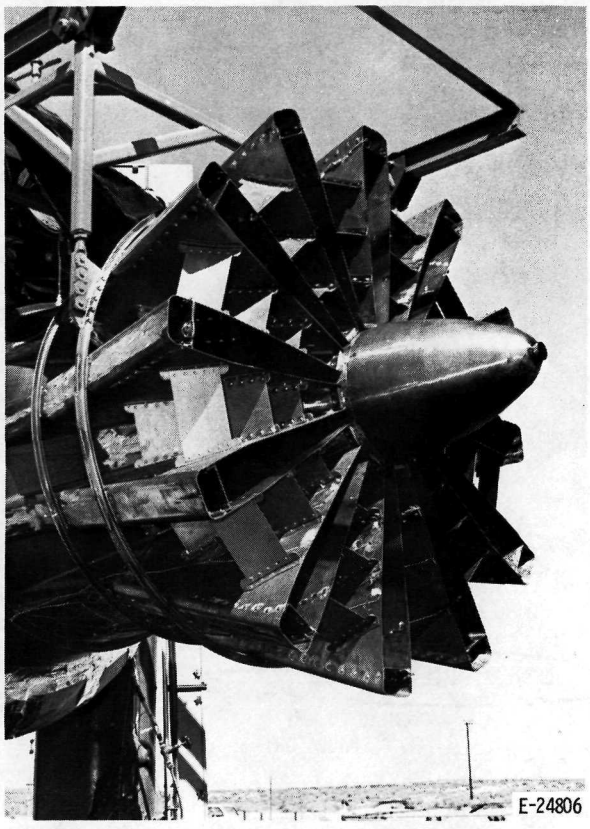

Figure 4. - Twelve-lobed velocity decayer nozzle.

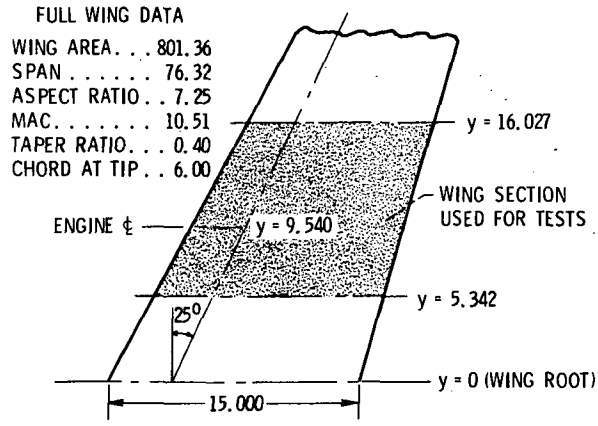

(a) SCHEMATIC OF WING SECTION.

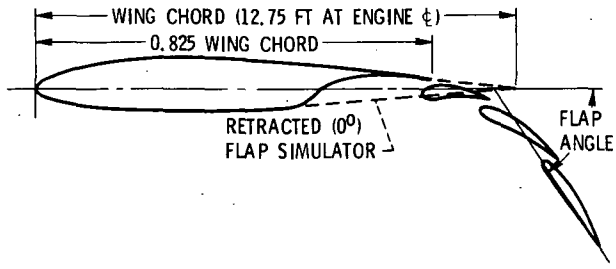

(b) TYPICAL CHORDWISE PROFILE THROUGH WING AND FLAPS.

Figure 5. - Wing and flap details. (All dimensions in ft)

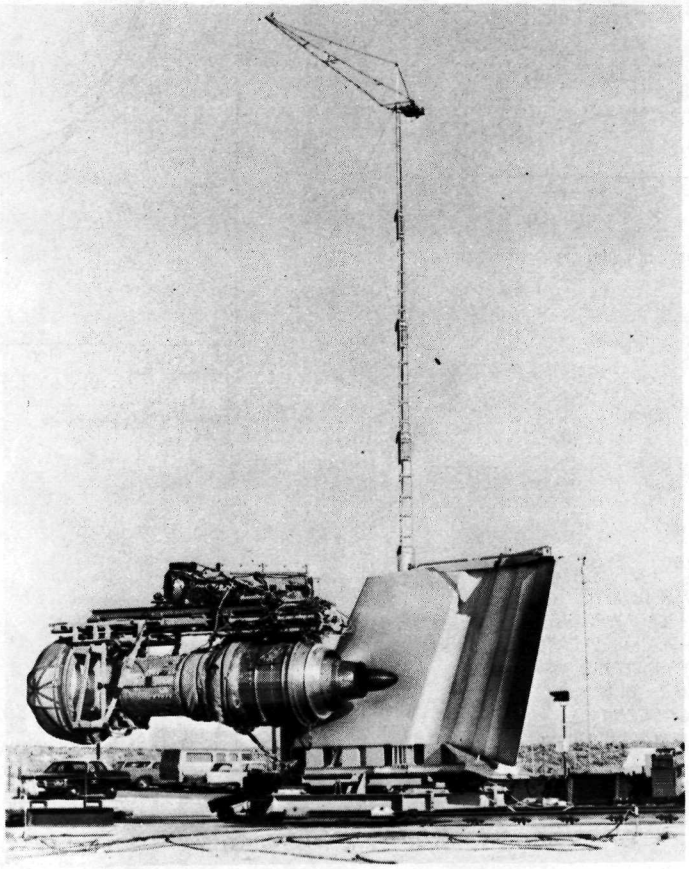

Figure 6. - Test installation at Edwards Air Force Base.

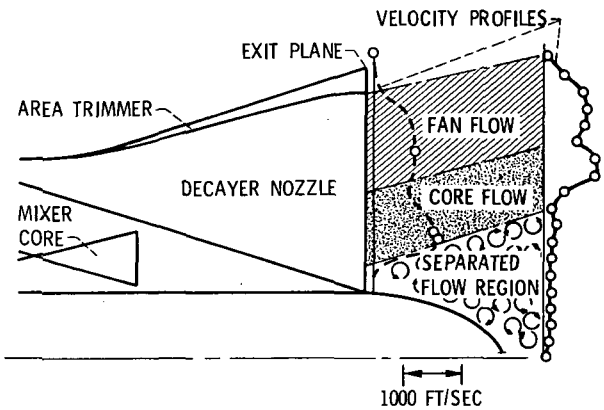

Figure 7. - Flow field at exit of lobe of mixer-decayer nozzle.

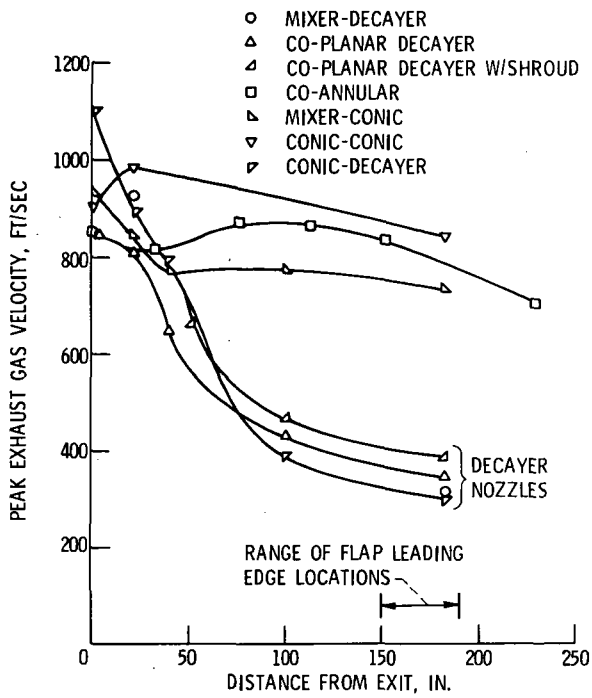

Figure 8. - Velocity decay characteristics at rated power.

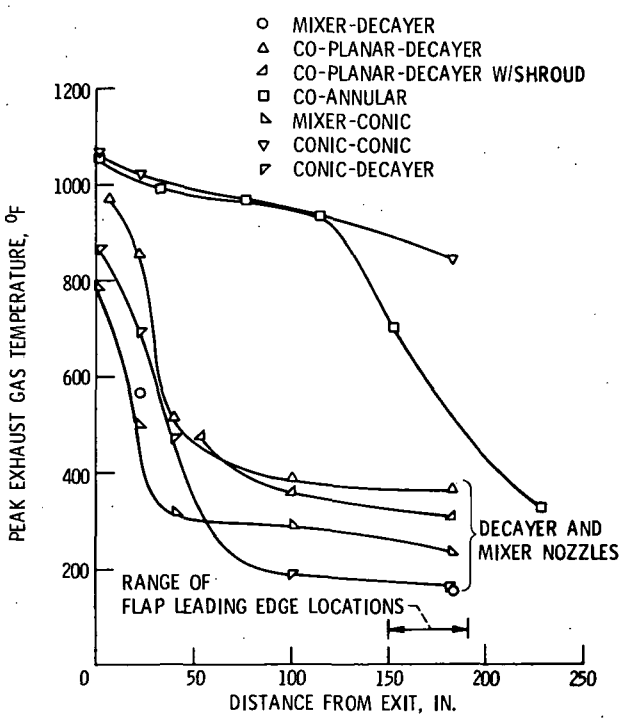

Figure 9. - Peak exhaust gas temperature decay at rated power.

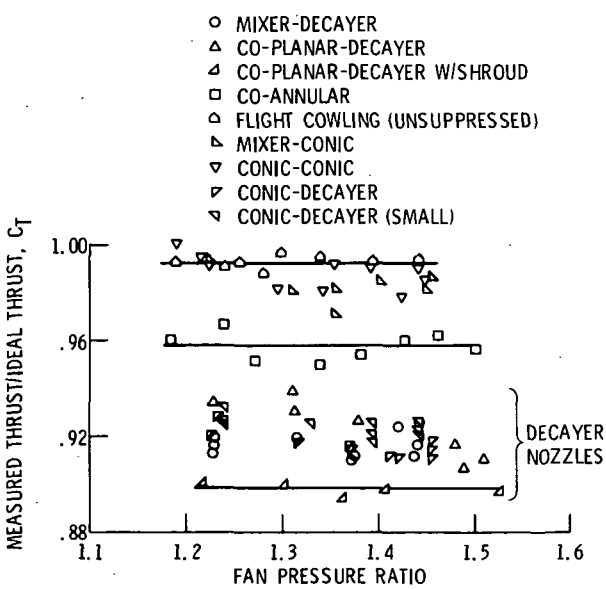

Figure 10. - Exhaust nozzle efficiency.

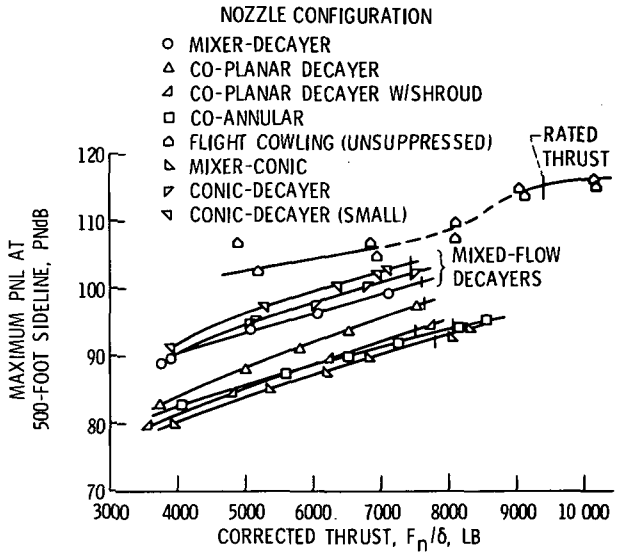

Figure 11. - TF34 noise comparison, engine alone.

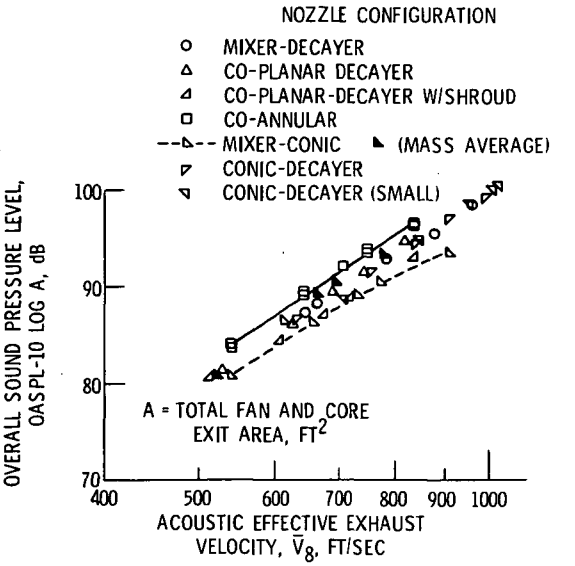

Figure 12. - OASPL noise comparison of various nozzles for engine alone. Radius, 100 ft; 130° from inlet.

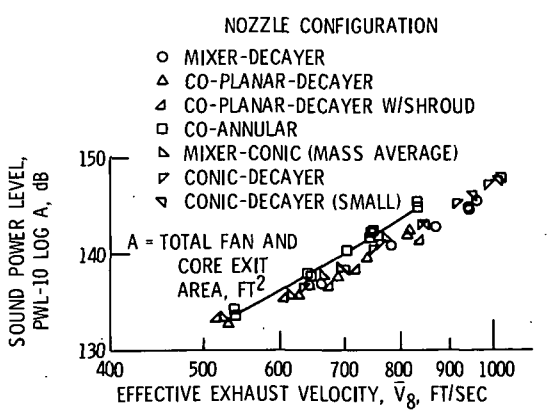

Figure 13. - Total normalized sound power of various exhaust nozzle systems for engine alone.

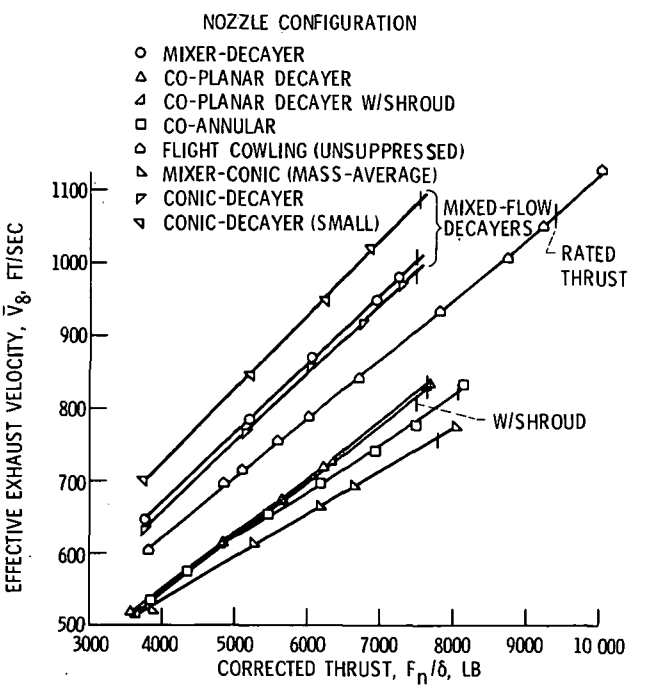

Figure 14. - Exhaust nozzle velocity comparisons.

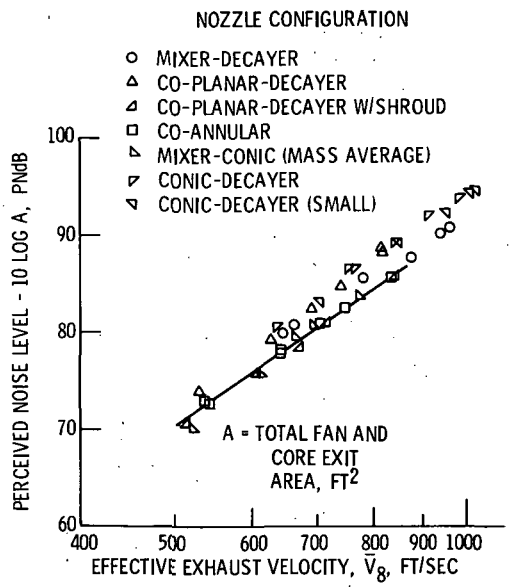

Figure 15. - Maximum normalized perceived noise at 500-foot sideline for engine alone.

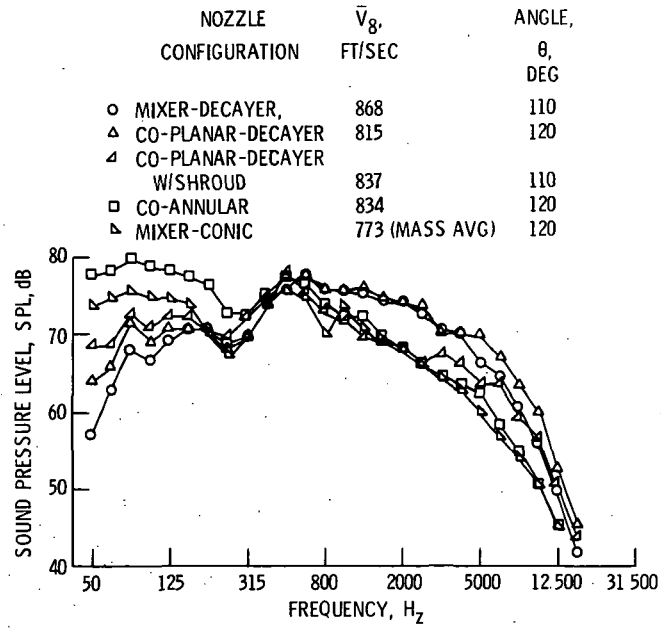

Figure 16. - 1/3-octave spectra at maximum PNL on 500-foot sideline for engine alone.

CONFIGURATION	x, IN.	y, IN.	z, IN. 0-20-40° FLAPS	z, IN. 15-35-55° FLAPS
MIXER-DECAYER	0	-45	183	165
CO-PLANAR DECAYER	0	-45	183	165
CO-PLANAR DECAYER W/SHROUD	0	-57	192	172
CO-ANNULAR	-12	-41	168	150

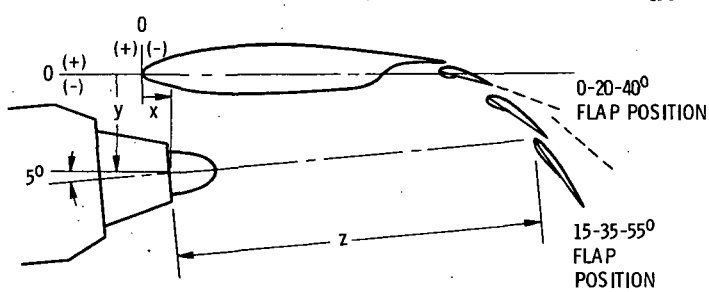

Figure 17. - Exhaust nozzle - wing orientation

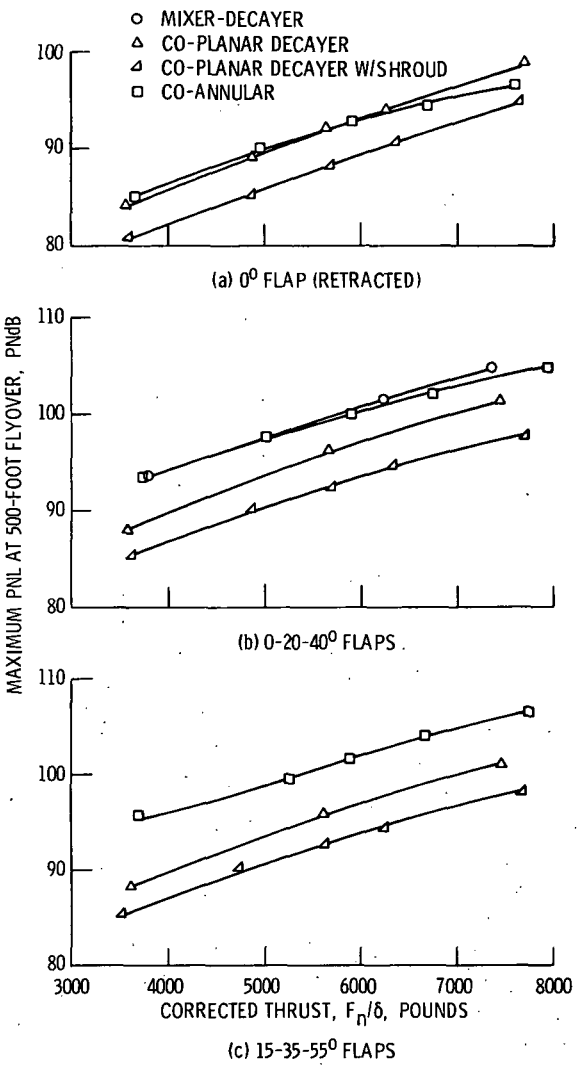

Figure 18. - Noise comparison of various powered lift exhaust nozzle systems.

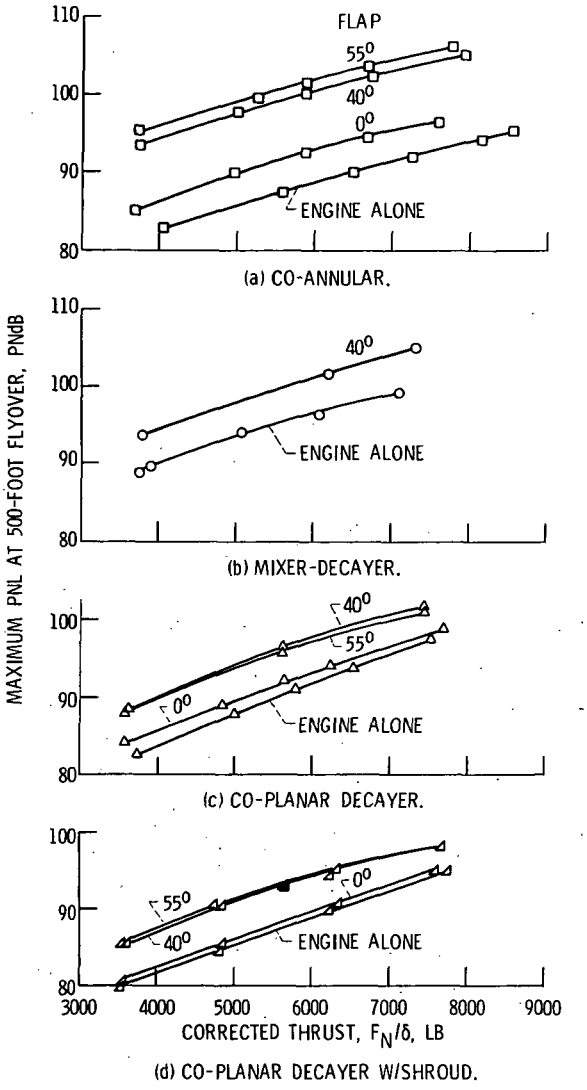

Figure 19. - Effect of powered lift on total flyover noise.

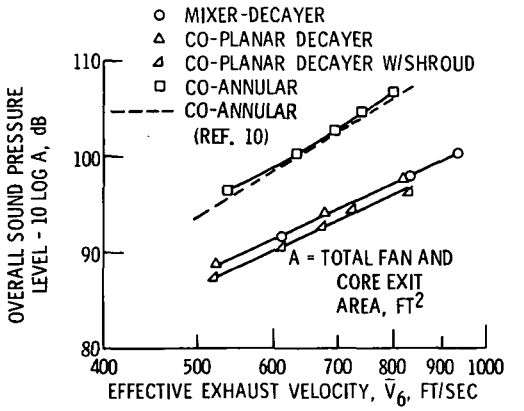

Figure 20. - Noise comparison of engine with 0-20-40^0 flaps 100 feet from nozzle exit and 80^0 from the inlet.

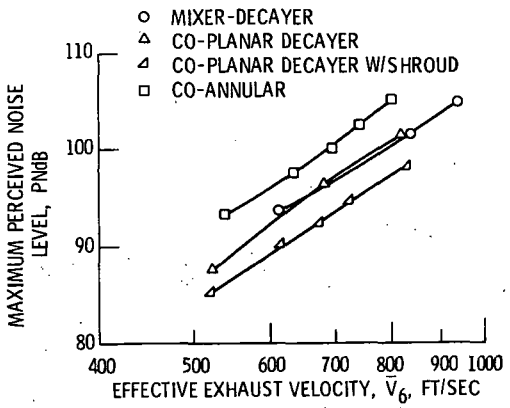

Figure 21. - Maximum perceived noise in a 500-foot flyover, engine with wing and 0-20-40° flaps.

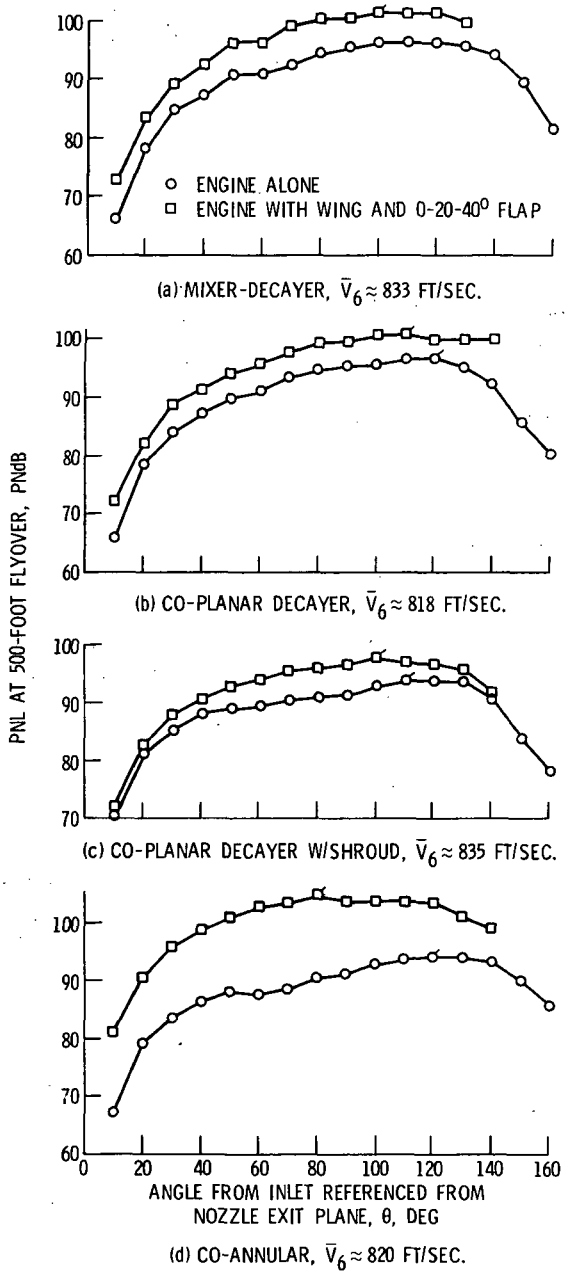

Figure 22. - Acoustic directivity characteristics in a 500-foot flyover.

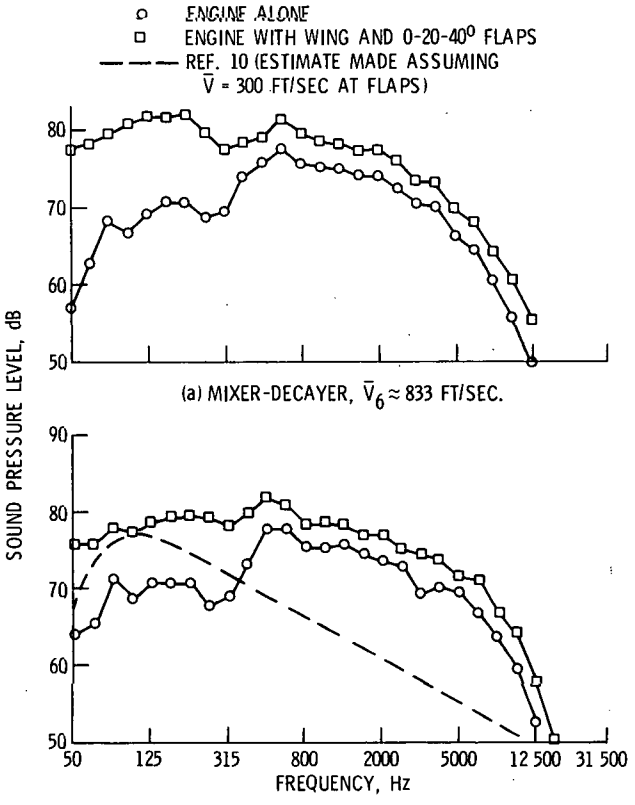

(a) MIXER-DECAYER, $\bar{V}_6 \approx 833$ FT/SEC.

(b) CO-PLANAR-DECAYER, $\bar{V} \approx 818$ FT/SEC.

Figure 23. - 1/3-Octave spectra at maximum PNL in 500-foot flyover.

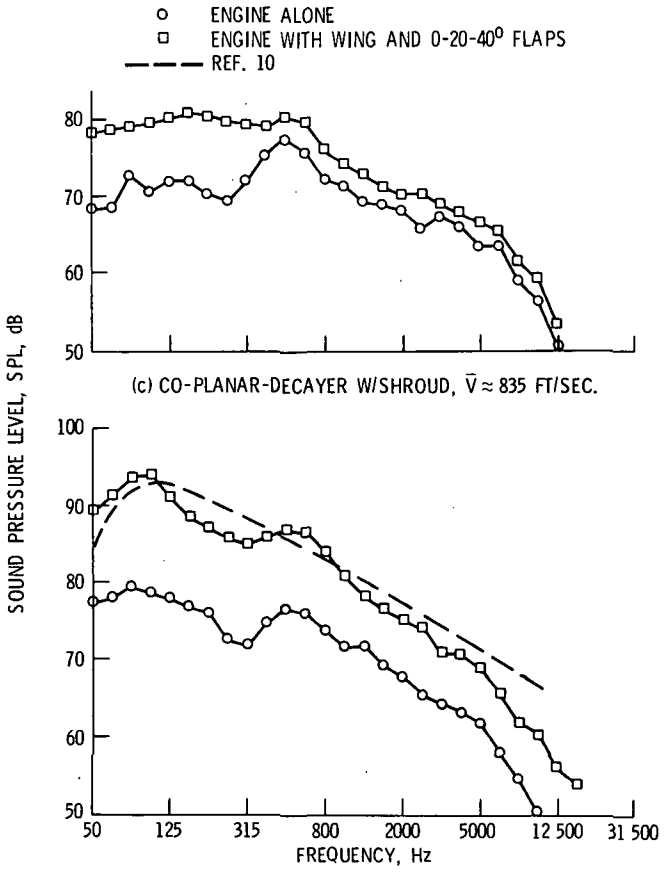

(c) CO-PLANAR-DECAYER W/SHROUD, $\bar{V} \approx 835$ FT/SEC.

(d) CO-ANNULAR, $\bar{V} \approx 820$ FT/SEC.

Figure 23. - Concluded.

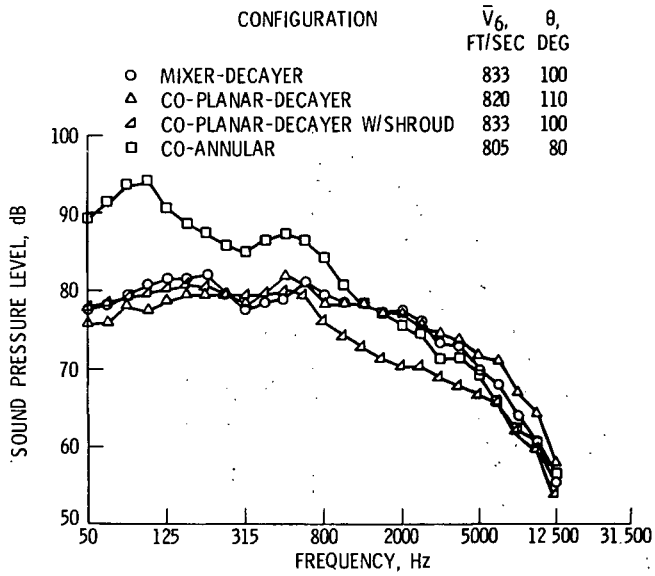

Figure 24. - 1/3-Octave spectra at maximum PNL in 500-foot flyover for engine with wing and 0-20-40° flaps.

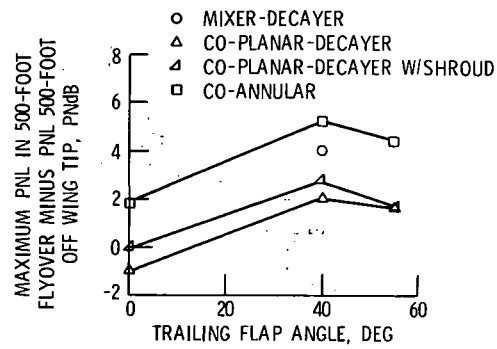

Figure 25. - Sideline relief from flyover flap noise at 500 feet.

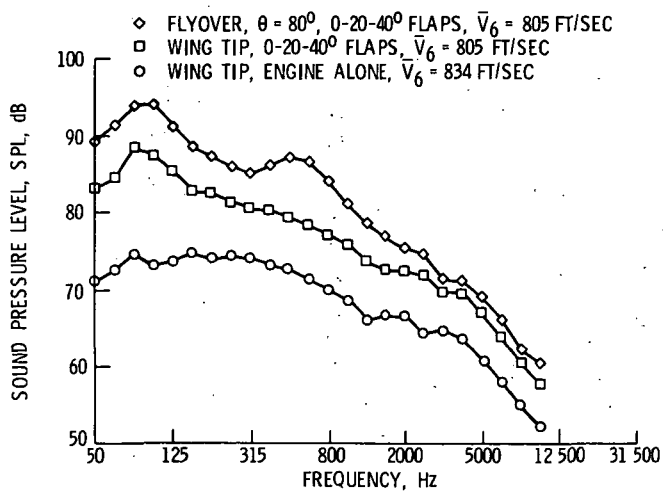

Figure 26. - Sound spectra at 500 foot wing tip-sideline compared to maximum 500-foot flyover, co-annular nozzle.